Multi-class traffic flow on a partially space-shared road

Yuan, Kai; Knoop, Victor L.; Hoogendoorn, Serge P.

DOI
10.1080/21680566.2019.1630689

Publication date
2019

Document Version
Final published version

Published in
Transportmetrica B

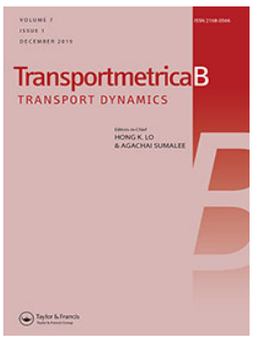

Taylor & Francis
Taylor & Francis Group

Transportmetrica B: Transport Dynamics

ISSN: 2168-0566 (Print) 2168-0582 (Online) Journal homepage: https://www.tandfonline.com/loi/ttrb20

Multi-class traffic flow on a partially space-shared road

Kai Yuan, Victor L. Knoop & Serge P. Hoogendoorn

To cite this article: Kai Yuan, Victor L. Knoop & Serge P. Hoogendoorn (2019) Multi-class traffic flow on a partially space-shared road, Transportmetrica B: Transport Dynamics, 7:1, 1505-1520, DOI: 10.1080/21680566.2019.1630689

To link to this article: https://doi.org/10.1080/21680566.2019.1630689

Published online: 20 Jun 2019.

TRANSPORTMETRICA B: TRANSPORT DYNAMICS
2019, VOL. 7, NO. 1, 1505–1520
https://doi.org/10.1080/21680566.2019.1630689

Taylor & Francis
Taylor & Francis Group

Multi-class traffic flow on a partially space-shared road

Kai Yuan, Victor L. Knoop and Serge P. Hoogendoorn

Department of Transport and Planning, Facility of Civil Engineering and Geoscience, Delft University of Technology, Delft, The Netherlands

ABSTRACT

Scarce urban space makes urban streets have to be partly shared by cars and cyclists. Traffic flow can be considerably influenced by cyclists, which are comparatively slower than cars. The fundamental diagram (FD) can change greatly, correlating to bike lane length and the cyclist flow. Models for the traffic dynamics on the space-shared streets are still lacking. This work fills the gap. This paper starts from proposing analytic formulas for the capacity, free-flow speed and critical density on a one-lane road, which together characterize the FD. The sensitivity of the FD to the bike lane length as well as the cyclist flow, using the analytical formulas, are presented. The given FD is satisfactory, compared with microscopic simulation results. Finally, we extend the research scope to a multi-lane road. It is expected that this work can benefit city designs and traffic operations.

ARTICLE HISTORY
Received 25 May 2018
Accepted 8 June 2019

KEYWORDS
Traffic flow; bike lane; moving bottleneck; fundamental diagram

1. Introduction

In urban environments most of which are car-centric cities, many negative trends of urbanization (e.g. noise, air pollution, low travel speed and unhealthy lifestyle) promote active travel modes (such as cycling). Traffic flow on streets is considerably influenced by cyclists by virtue of the comparatively low speed.

Since urban space is scarce, new bike lane (or cycle lane) building is not straightforward. Moreover, bike lanes might also limit the use of roads for other travel modes. Hence, it may not be efficient to build bike lanes covering a whole city even though this may be the best for cyclists. Even in the Netherlands where 53% of trips are by bicycles in 2010, engineers are considering to let cyclist share roads with cars on more and more streets. Hence, it is desirable to study the influence of cyclist flow on the traffic flow, which will contribute to practical applications in the city design and operations.

If cyclists ride along a bike lane all the time, fully segregated from passenger cars on streets, the only interruptions where vehicles would need to stop due to crossing cyclists, are the same as described for pedestrian crossings (see HCM 2016, Daganzo and Knoop 2016 and Knoop and Daganzo 2017 for impacts of pedestrian crossings on traffic flow on streets), otherwise there will be no interaction at all. Hence, this paper narrows the research interest to the scenario where streets are partially shared by cyclists (including the fully shared case).

When cyclists ride on the lane shared with passenger cars, cyclists play a role of moving bottlenecks. The fundamental diagram (especially the street capacity, free-flow speed as well as critical density) of the car traffic will be influenced by the interactions with cyclist flow. Therefore, the impacts of cyclists on traffic flow depend on the extent the bike lane covers the street (in the longitudinal direction) and the cyclist flow characteristics (flow, density and speed).

CONTACT Kai Yuan spidermanyuan@gmail.com

Knowledge about the influence of bike lane proportion and the cyclist flow on the traffic flow, which can benefit traffic modeling and traffic operations, however as far as authors know, is still missing. This paper tries to fill in the gap. We firstly study the fundamental diagram on a one-lane ring road where vehicles are not allowed to overtake cyclists on the shared lane. This paper calls this one-lane ring road case a no-overtaking case. Notice that in the no-overtaking case, when cyclists ride on the bike lane, passenger cars can overtake cyclists. Close-form formulations are proposed to show how the traffic fundamental diagram (FD) is determined by the bike lane proportion and the cyclist flow. We extend the research on the one-lane road to a multi-lane road case. On a multi-lane road, passenger cars can overtake cyclists on the shard road section at any locations.

We believe that the analysis performed in this paper can also hold generically for roads with heterogeneous road users. After reviewing previous works focusing on multi-class traffic flow modeling (van Wageningen-Kessels 2013, 2016) and studies on moving bottlenecks (Munoz and Daganzo 2002; Wong and Wong 2002; Laval and Carlos 2006; Laval 2006a, 2006b, 2009; Leclercq, Laval, and Chiabaut 2011; Coifman 2015; Chen et al. 2016), we see that insights in this work also can be applied to understand the traffic flow dynamics on roads where the slow road users (e.g. heavy trucks or buses) are partially segregated from fast road users (e.g. passenger cars) in space.

This paper is organized as follows. Section 2 describes the studied scenario and flow characteristics, corresponding to traffic flow kinematic wave theory. Sections 3 and 4 present the formula of the capacity and the free-flow speed for the FD, respectively. In Section 5, we formulate the critical density in Section 5.1 and the wave speed in Section 5.2, following which the FD approximation formula is given in Section 5.3. Section 6 presents simulation results which is compared with analytical FD approximations. In Section 7, extensions to multi-lane road structure are discussed. Finally, this paper finishes with conclusions and discussions in Section 8.

2. Problem description

This section aims to simplify the studied problem and list assumptions.

Consider a one-lane ring road with total length L, see Figure 1(a). The road is shared by two categories of users, i.e. fast traffic and slow traffic, unless a segregated slow traffic lane, with length L_s, is built. The slow traffic lane may represent the bike lane (as in this paper), the truck-only lane, or any other lanes designed to separate the slow traffic from other prevailing traffic stream for a certain distance. In this research, the fast traffic is the passenger car, while the slow traffic is the cyclist. Only cyclists are allowed to use the bike lane.

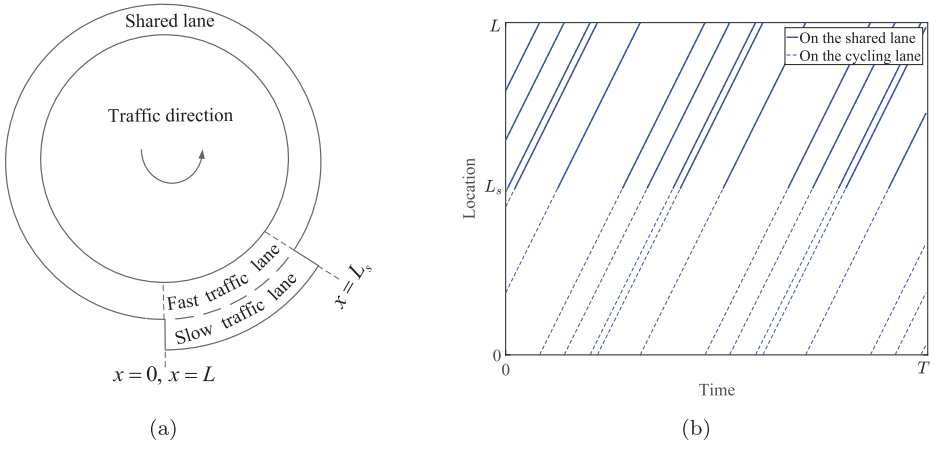

Figure 1. The studied ring road structure and an example of moving bottleneck trajectories. (a) A ring road with a segregated slow traffic (cyclist) lane. (b) Trajectories of moving bottlenecks.

Cyclists are much slower than passenger cars. The x is the distance from the original point, increasing in the traffic direction. An x–t plot is shown in Figure 1(b), where the solid and dotted lines denote the trajectories of cyclist on the shared lane and the bike lane, respectively. The cyclists are absent on the shard lane when $x \in [0, L_s)$, moving on the bike lane. Figure 1(a) shows that on the shared lane no overtaking is allowed. In this no-overtaking case, passenger cars can only pass cyclists where a bike lane is built. In Section 7, an extension to multi-lane road where passenger cars can overtake cyclists on the passing lanes is discussed. To describe the cyclist, two parameters, i.e. their intrinsic free flow speed v_s and entering flow q_s, suffice. Please note that v_s and q_s are predefined as constants in this research, i.e. independent of the passenger car density. As the passenger car density increases, the proportion of cyclists decreases.

Several assumptions in this research are listed as follows:

- Assumption 1: Vehicles are treated as a stream of cars. Traffic is characterized by flow, density and speed. The passenger car is characterized by a triangular fundamental diagram, with capacity c, jam density k_j and wave speed w. The free flow speed v_f and critical density k_c can be derived from these three parameters.
- Assumption 2: Cyclists on the shared lane are simplified as moving bottlenecks for cars. Queues of passenger cars form in the upstream of moving bottlenecks, the evacuation of which starts when the leading cyclist move to the cyclist lane. When the vehicular density k on streets are so high that the corresponding vehicular speed v is not higher than the cyclist speed v_s (i.e. when $k = k_0$, the vehicular speed $v = v_s$), the cyclists are not moving bottlenecks anymore. The fundamental diagram within density range $[k_0, k_j]$ is the same as the triangular fundamental diagram given by jam density k_j and wave speed w. In this paper, the focus of the research is narrowed to the passenger car density upper bounded by $k_0 = k_j w/(v_s + w)$. That is, only density $k \in [0, k_0]$ is considered.
- Assumption 3: The space occupied by the cyclist is assumed to be zero. When describing cyclist flow, we do not consider cyclist flow dynamics (e.g. lateral interactions between cyclists and cyclist heterogeneity), which differs from literature focusing on studying cyclist behaviors (e.g. Hoogendoorn and Daamen 2016). That is, the cyclist always moves at its free-flow speed.
- Assumption 4: Cyclists enter the ring road randomly. The time-headway between two successive cyclists should follow an exponential distribution, always positive. The stochastic process is considered in this research.

Approximating the FD requires four parameters – free-flow speed, capacity, critical density and wave speed at density k_0. This work is going to present closed-form expressions of these four additional parameters, prior to giving an FD formula. Simulations are conducted to see whether all proposed closed-form expressions can fit simulation results.

Because dimensional analysis can eliminate constants, and facilitate finding independent parameters interpreting results, we plan to use dimensionless parameter to describe the problem. In this study, three dimensions ($\hat{u}_t = L_s/v_s$, $\hat{u}_s = cL_s/(v_s k_j)$ and $\hat{u}_n = cL_s/v_s$) are chosen. So the flow, speed and density will be measured with unit c, c/k_j and k_j, respectively. Please notice that parameters c, v_s, k_j, w are

Table 1. List of symbols.

Parameter	Dimensionless parameter	Value	Meaning
L_s	$\hat{L}_s$	$v_s k_j/c$	Cycling lane length
L	$\hat{L}$	$Lv_s k_j/(cL_s)$	Ring road length
v_s	$\hat{v}_s$	$v_s k_j/c$	Cyclist speed
k_j	$\hat{k}_j$	1	Traffic jam density
w	$\hat{w}$	wk_j/c	Shock wave speed
c	$\hat{c}$	1	Traffic capacity
q_s	$\hat{q}_s$	q_s/c	Entering cyclist flow

predefined to describe traffic flow characteristics, so the cycling lane length $\hat{L}_s = v_s k_j / c$ is invariable. In a special case where $v_s k_j = c$, we can see that $\hat{L}_s = 1$, and $1/\hat{L} = L_s/L$ indicating the proportion of cycling lane length to total street length. With dimensionless analysis, all parameters are transformed into dimensionless number (signaled by a hat), see Table 1.

3. Capacity

Capacity here means the maximum stationary traffic flow passing one fixed point on the ring road. The dimensionless capacity is described by $\hat{\mathbf{C}}$. In this paper, parameters of the externally given FD are formatted in boldface.

In principle, the FD can be constructed by deriving tight 'cuts' associated to all valid moving observer speeds ($\hat{u}$) (Daganzo and Geroliminis 2008). Each cut is a linear cost function $f(\hat{k}) = \hat{\Delta} + \hat{k} \cdot \hat{u}$ where $\hat{\Delta}$ is the cost of traffic flow in variational theory (Daganzo 2005), see Figure 2. When the moving observer is moving at speed $\hat{u}$, the maximum flow passing the moving observer is denoted as $\hat{\Delta}$. That is, each moving observer speed $\hat{u}$ corresponds to a linear cut. The FD is the lower envelop of all cuts. So the capacity can be predicted by estimating the minimum $\hat{\Delta}$ with $\hat{u} = 0$ km/h. This 'cut' approach is what we apply to find the capacity. Consider a so-called moving observer. This observer will travel at the location where the passenger cars and the cyclists share the infrastructure via a path shown in Figure 3. To find the tightest boundary, this section defines the moving observer's path character as follows:

- The observer always starts traveling at location $\hat{x} = \hat{L}$ and at time when a moving bottleneck enters the slow traffic lane.
- The observer always ends the travel at the starting location (or origin) $\hat{x} = \hat{L}$ to ensure $\hat{u} = 0$ km/h.
- The observer travels at speed $-\hat{w}$ until meeting a moving bottleneck or arriving at location $\hat{x} = \hat{L}_s$.
- When the observer meets a moving bottleneck, it starts traveling at speed $\hat{v}_s$ until arriving $\hat{x} = \hat{L}$.
- When the observer arrives at location $\hat{x} = \hat{L}_s$, it waits at the same position until when a moving bottleneck passes.
- This way, when the moving observer returns to the origin, it starts traveling upstream again.

Hence, we can find two categorizes of paths (i.e. path 1 and path 2 in Figure 3). When traveling on path 1 ($M_1 \rightarrow M_2 \rightarrow M_3$), the moving observer will meet a cyclist before reaching $\hat{x} = \hat{L}_s$ and return to $x = \hat{L}$. While traveling on path 2 ($M_3 \rightarrow M_4 \rightarrow M_5 \rightarrow M_6$), the moving observer will arrive at location

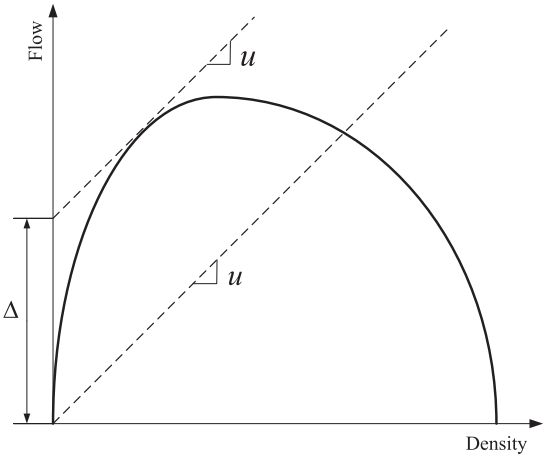

Figure 2. Approximating fundamental diagram using tight cuts.

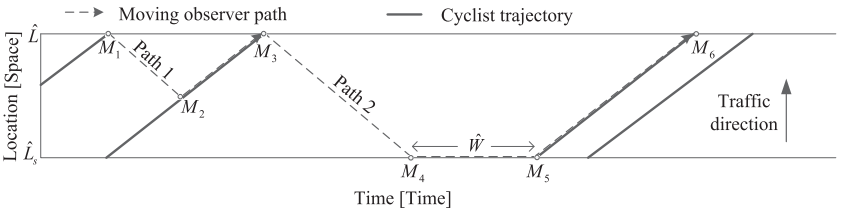

Figure 3. Trajectories of moving observers and valid paths for capacity estimation.

$\hat{x} = \hat{L}_s$, and wait until a cyclist enters. Following the cyclist trajectory, the moving observer will go back to the starting location. The relative capacity detected by the observer on path 1 is denoted by $\hat{C}_1$, meaning the flow passing the moving observer on path 1. On the path 1 (which is a round trip) the moving observer passes no vehicle when traveling downstream (upward) at speed $\hat{v}_f$, while the cost on the downward trip is $\hat{w}\hat{k}_j$. Hence, the total number of vehicles passing the moving observer on path 1 should be $\hat{k}_j\hat{r}$ (unit $[\hat{u}_n]$) within $\hat{r}/\hat{w} + \hat{r}/\hat{v}_s$ (unit $[\hat{u}_t]$), where $\hat{r}$ is the one-way trip distance traveled by the observer (with unit $[\hat{u}_s]$). That is, the capacity on path 1 is $\hat{C}_1 = \hat{w}\hat{v}_s/(\hat{w} + \hat{v}_s)$, regardless of $\hat{r}$. The capacity on path 2 $\hat{C}_2$ is related to the time duration (denoted by $\hat{W}$ and named as 'waiting time' from now on) during which the observer waits at $x = \hat{L}_s$. Let us assume that the moving bottleneck enters randomly (as in Assumption 4). So the time headway between two moving observers shows an exponential distribution, with expected value $\mathrm{E}[\hat{h}_s] = 1/(\hat{q}_s\hat{u}_n)$. $\mathrm{E}[\cdot]$ denotes the expected value. On path 2, the waiting time has an expected value $\mathrm{E}[\hat{W}] = \mathrm{E}[\hat{h}_s]$. When the moving observer travels upstream on path 2, the total passing vehicle number is $\hat{k}_j(\hat{L} - \hat{L}_s)$. When the moving observer waits for $\mathrm{E}[\hat{W}]$, the passing vehicle number is $\hat{c}\mathrm{E}[\hat{W}]$ (unit $\hat{u}_n$). The total travel time (with unit $\hat{u}_t$) on path 2 is $(\hat{L} - \hat{L}_s)(1/\hat{v}_s + 1/\hat{w}) + \mathrm{E}[\hat{W}]$. Hence we can have the mean capacity detected on the path 2 as $\mathrm{E}[\hat{C}_2] = (\hat{k}_j(\hat{L} - \hat{L}_s) + \hat{c}\mathrm{E}[\hat{W}])/((\hat{L} - \hat{L}_s)(1/\hat{v}_s + 1/\hat{w}) + \mathrm{E}[\hat{W}])$.

The probability that the observer moves on path 1 and 2 is denoted by P_1 and P_2, respectively. $\mathrm{P}_1 = \mathrm{P}(\hat{h}_s \leqslant \hat{H}_s)$ and $\mathrm{P}_2 = 1 - \mathrm{P}_1$, where $\hat{H}_s = (\hat{L} - \hat{L}_s)(1/\hat{w} + 1/\hat{v}_s)$. The mean street capacity $\hat{\mathbf{C}}$ can be given by $\mathrm{E}[\hat{\mathbf{C}}] = \mathrm{P}_1\hat{C}_1 + \mathrm{P}_2\mathrm{E}[\hat{C}_2]$. Since $\mathrm{P}(\hat{h}_s \leqslant \hat{H}_s) = 1 - \mathrm{e}^{-\hat{q}_s\hat{H}_s\hat{u}_n}$, we can have $\mathrm{E}[\hat{\mathbf{C}}]$ as

$$\mathrm{E}[\hat{\mathbf{C}}] = \left[1 - \mathrm{e}^{-\beta_1\beta_2\hat{u}_n}\right]\frac{1}{\beta_1} + \mathrm{e}^{-\beta_1\beta_2\hat{u}_n}\frac{1 + \beta_2\hat{u}_n}{\beta_1\beta_2\hat{u}_n + 1} \tag{1}$$

where $\beta_1 = 1/\hat{w} + 1/\hat{v}_s$ and $\beta_2 = \hat{q}_s(\hat{L} - \hat{L}_s)$.

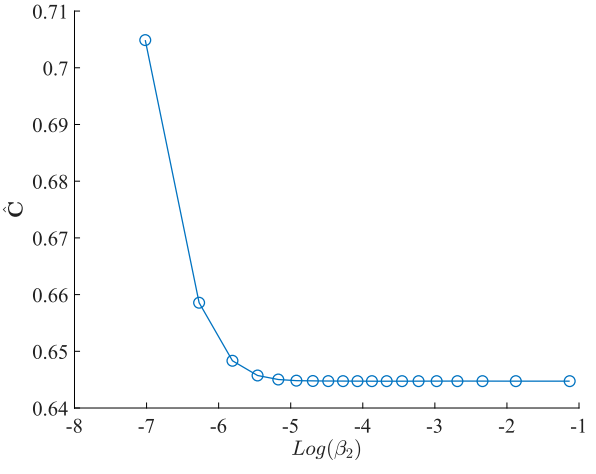

Figure 4. Sensitivity of street capacity to the β_2.

Equation (1) shows that the capacity $\hat{\mathbf{C}}$ is a function of one parameter, β_2. It is worthwhile to notice that β_2 indicates the total distance traveled by cyclists on the shared lane in one-time unit. The unit of β_2 is $[c\hat{u}_s]$. The increase of β_2 can be seen as a result of an increase of cyclist flow (q_s) or a reduction in the proportion of bike lane length (L_s/L). As long as β_2 is constant, the capacity should be constant. Figure 4 presents the capacity with different β_2. For a clear presence, the lateral axis is the logarithm of $\hat{L}$, which rises as β_2 increases. It is shown in Figure 4 that the capacity decreases as β_2 increases, and that the capacity will tend to flatten at around $\hat{v}_s\hat{k}_0$.

4. Free flow speed

This section studies the free flow speed $\hat{\mathbf{V}}_f$ in the studied ring road. Consider a case that except moving bottlenecks, only one vehicle (fast traffic) is traveling from $x = 0$ to $x = \hat{L}$. With a certain probability, the vehicle will come across a moving bottleneck, encountering traffic delays. Hence, the free-flow speed $\hat{\mathbf{V}}_f$ is defined as the average vehicular speed when the prevailing passenger car density is around zero.

Before arriving at $x = \hat{L}_s$, the vehicle is driving at speed $\hat{v}_f$. In Figure 5, one circle, denoted by 'A', is the time when the vehicle arrives at $x = \hat{L}_s$. $\hat{W}_a$ is the time duration for which last moving bottleneck has been away from there when the vehicle arrives. If $\hat{W}_a \geqslant \hat{d}_{\max}$, there is no delay; or the vehicle will be delayed by $\hat{\tau}$. For calculating the free flow speed, we only need to calculate the probability of being delayed and the average delay on condition of $\hat{W}_a < \hat{d}_{\max}$. The delay can be approximated by the following equation:

$$\mathrm{E}[\hat{\tau}] = P(\hat{W}_a < \hat{d}_{\max}) \cdot (\hat{d}_{\max} - \mathrm{E}[\hat{W}_0]) \tag{2}$$

where $\mathrm{E}[\hat{W}_0]$ is the average $\hat{W}_a$ on condition $\hat{W}_a < \hat{d}_{\max}$. Readers can verify that $\hat{W}_a$ shows an exponential distribution with $\mathrm{E}[\hat{W}_a] = 1/(\hat{q}_s\hat{u}_n)$. So $P(\hat{W}_a < \hat{d}_{\max}) = 1 - \mathrm{e}^{-\hat{q}_s\hat{d}_{\max}\hat{u}_n} - P(\hat{W}_a < \hat{d}_{\max})$ where the probability $P(\hat{W}_a = \hat{d}_{\max}) \approx 0$ According to

$$\mathrm{E}[W_0] = \int_0^{d_{\max}} \left[1 - \left(1 - \mathrm{e}^{-q_s y}\right) / \left(1 - \mathrm{e}^{-q_s d_{\max}}\right)\right] \mathrm{d}y \tag{3}$$

we can have $\mathrm{E}[\hat{W}_0]$ as

$$\mathrm{E}[\hat{W}_0] = \frac{-\hat{d}_{\max}\hat{q}_s\hat{u}_n + \mathrm{e}^{\hat{d}_{\max}\hat{q}_s\hat{u}_n} - 1}{(\mathrm{e}^{\hat{q}_s\hat{d}_{\max}\hat{u}_n} - 1)\hat{q}_s\hat{u}_n} \tag{4}$$

Combining (2) and (4), we can give a closed-form expression of $\mathrm{E}[\tau]$. Since the free flow speed can be estimated as $\mathrm{E}[\hat{\mathbf{V}}_\mathbf{f}] = \hat{L}/(\hat{L}/\hat{v}_f + \mathrm{E}[\tau])$, we can have

$$\mathrm{E}[\hat{\mathbf{V}}_\mathbf{f}] = \frac{\hat{L}}{\frac{\hat{L}}{\hat{v}_f} + (1 - \mathrm{e}^{-\hat{q}_s\hat{d}_{\max}\hat{u}_n})\left[\hat{d}_{\max} - \frac{-\hat{d}_{\max}\hat{q}_s\hat{u}_n + \mathrm{e}^{\hat{d}_{\max}\hat{q}_s\hat{u}_n} - 1}{(\mathrm{e}^{\hat{q}_s\hat{d}_{\max}\hat{u}_n} - 1)\hat{q}_s\hat{u}_n}\right]} \tag{5}$$

where $\hat{d}_{\max} = (\hat{L} - \hat{L}_s)(1/\hat{v}_s - 1/\hat{v}_f)$. (5) is affected by two external parameters, including $\hat{q}_s$ and $\hat{L}$. When cyclists are fully served by a bike lane on the ring road (i.e. $L_s = L$ or $\hat{L} = v_s k_j/c \approx 1.36$), the

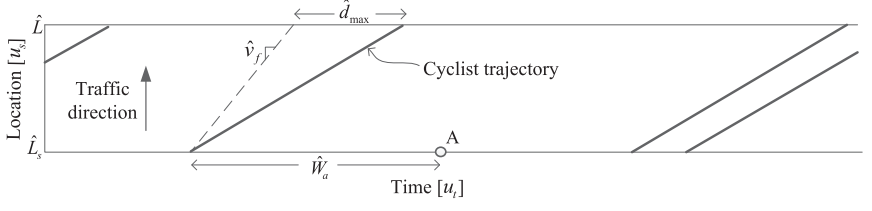

Figure 5. Free flow speed estimations.

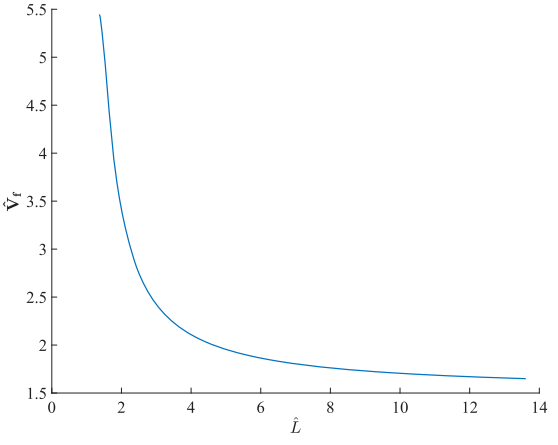

Figure 6. Sensitivity of street free-flow speed to the $\hat{L}$.

free-flow speed equals vehicular free-flow $\hat{v}_f$ (i.e. $\hat{\mathbf{V}}_\mathbf{f} \approx 5.44$). In (5), $\hat{L}$ is restricted within a range of $[1.36, +\infty)$. Figure 6 shows the relation between the free-flow speed $\hat{\mathbf{V}}_\mathbf{f}$ and $\hat{L}$. As the bike lane proposition decreases, the free-flow speed $\hat{\mathbf{V}}_\mathbf{f}$ decreases and finally tend to flatten at around 1.5.

5. Fundamental diagram

This section aims to give the macroscopic fundamental diagram. We firstly derive the expression for the critical density in Section 5.1, following which we estimate the wave speed at density $\hat{k}_0$ in Section 5.2. Finally, combining the capacity and the free-flow speed estimated in previous sections, Section 5.3 present the expression for the FD approximation.

5.1. Critical density

In order to estimate the critical density $\hat{\mathbf{K}}_c$, we firstly limit the cut slope $\hat{v}_{\text{cut}}$ within a range of $[0, \hat{L}/(\hat{L}_s/\hat{v}_f + (\hat{L} - \hat{L}_s)/\hat{v}_s))$. Secondly we construct a path $O \to D_1 \to D_2 \to D$ (see Figure 7(a)) that is able to give the minimum cost $\hat{\Delta}_{OD}$. In Figure 7(a), the moving observer travels from 'O' to 'D'. The slope of the line connecting 'O' and 'D' is $\hat{v}_{\text{cut}}$. The minimum cost for traveling from 'O' to 'D' is denoted by $\hat{\Delta}_{OD}$. The cost from O to D_1, as well as from D_2 to D are zero. The expected value of the minimum cost between D_1 and D_2, which is denoted by $\hat{\Delta}_{D_1D_2}$, is $\mathrm{E}[\hat{\mathbf{C}}]$. Hence, we can formulate $\hat{\Delta}_{OD} = \hat{\Delta}_{D_1D_2} \cdot \hat{t}_{D_1D_2}/\hat{t}_{OD}$, where $\hat{t}_{D_1D_2} = \hat{t}_{OD} - \hat{t}_{OD_1} - \hat{t}_{D_2D}$, $\hat{t}_{OD} = \hat{L}/\hat{v}_{\text{cut}}$, $\hat{t}_{OD_1} = \hat{L}_s/\hat{v}_f$ and $\hat{t}_{D_2D} = (\hat{L} - \hat{L}_s)/\hat{v}_s$ are the time duration from D_1 to D_2, from O to D, from O to D_1 and from D_2 to D, respectively. Hence, we can express $\hat{\Delta}_{OD}$ as

$$\mathrm{E}[\hat{\Delta}_{OD}] = \mathrm{E}[\hat{\mathbf{C}}] + \frac{\mathrm{E}[\hat{\mathbf{C}}] \cdot \hat{v}_{\text{cut}}}{\hat{L}} \left(-\frac{\hat{L}}{\hat{v}_s} - \frac{\hat{L}_s}{\hat{v}_f} + \frac{\hat{L}_s}{\hat{v}_s} \right) \tag{6}$$

Of any straight line, we denote the costs for the cuts by $\mathrm{E}[\hat{\Delta}_{OD}]$. Every cut can be formulated as $R(\hat{v}_{\text{cut}}, \hat{k}) = \mathrm{E}[\hat{\Delta}_{OD}] + \hat{k} \cdot \hat{v}_{\text{cut}}$. If the FD free-flow branch can be approximated by m cuts (m is a positive integer), the ith cut is denoted by $R^i(\hat{v}^i_{\text{cut}}, \hat{k})$, $i = 1, 2 \cdots m$ and $\hat{v}^i_{\text{cut}}$ is the slope of the ith cut. When two cuts R^i and R^j intersect at $\hat{k}^{ij}$ ($i, j = 1, 2 \cdots m$ and $i \neq j$), $R^i(\hat{v}^i_{\text{cut}}, \hat{k}^{ij}) = R^j(\hat{v}^j_{\text{cut}}, \hat{k}^{ij})$. Readers can verify that $\hat{k}^{ij} = \frac{\mathrm{E}[\hat{\mathbf{C}}]}{\hat{L}} \left(\frac{\hat{L}}{\hat{v}_s} + \frac{\hat{L}_s}{\hat{v}_f} - \frac{\hat{L}_s}{\hat{v}_s} \right)$ which is a constant. If all cuts intersect, this yields a capacity point. Hence, the

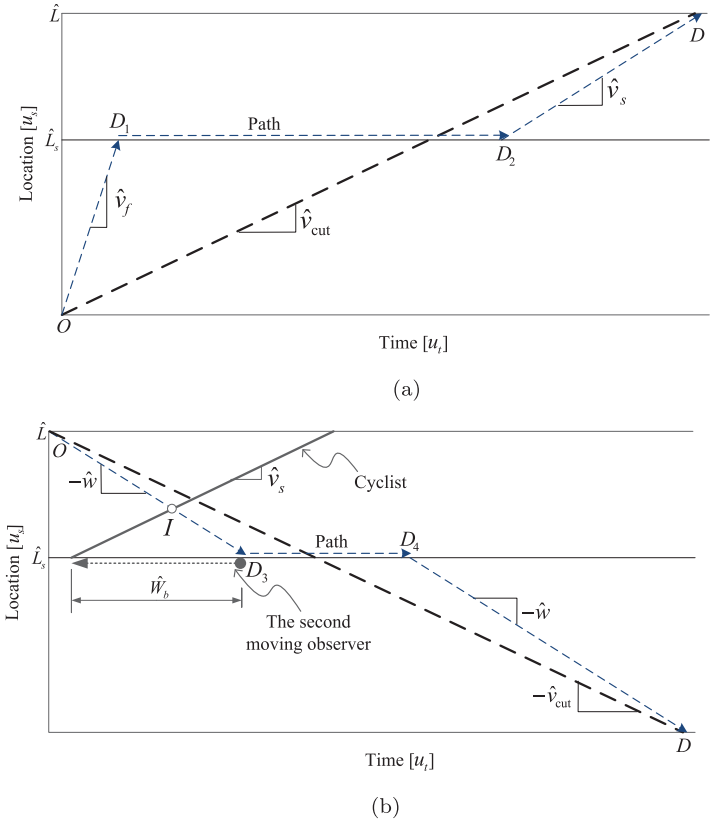

Figure 7. Trajectories of moving observers and valid paths for minimum cost estimation. (a) Moving observer moves forward. (b) Moving observer moves backward.

critical density $\hat{\mathbf{K}}_c$ of the FD can be given as

$$\hat{\mathbf{K}}_c = \frac{\mathrm{E}[\hat{\mathbf{C}}]}{\hat{L}} \cdot \left(\frac{\hat{L}}{\hat{v}_s} + \frac{\hat{L}_s}{\hat{v}_f} - \frac{\hat{L}_s}{\hat{v}_s} \right) \tag{7}$$

Remark that the cut series cannot be directly used for shaping the free-flow branch. We explain as follows. Recall that in (6), the cost $\mathrm{E}[\hat{\Delta}_{OD}]$ is calculated by assuming $\mathrm{E}[\hat{\Delta}_{D_1D_2}] = \mathrm{E}[\hat{\mathbf{C}}]$. However, this approximation can be the nearest when the time duration $\hat{t}_{D_1D_2}$ is infinite (i.e. $\hat{v}_{\text{cut}} \to 0$) because $\mathrm{E}[\hat{\mathbf{C}}]$ is a result of the stochastic process of the moving bottlenecks. When $\hat{v}_{\text{cut}} > 0$, the moving observer can only experience cost $\mathrm{E}[\hat{\mathbf{C}}]$ when traveling at mean speed 0 (i.e. from D_1 to D_2) after meeting a first cyclist. Before that the cost borne by the waiting moving observer at location $\hat{x} = \hat{L}_s$ should be $\hat{c} = 1$ for a time duration (denoted by $\hat{W}_1$). Prior to reaching the destination D, after meeting the last cyclist, the cost borne by the moving observer should also be $\hat{c} = 1$ for a time duration $\hat{W}_2$. Since both $\hat{W}_1$ and $\hat{W}_2$ follow an exponential distribution with the expected value $1/(\hat{q}_s\hat{u}_n)$ which is a constant, the moving observer will experiences the cost $\mathrm{E}[\hat{\mathbf{C}}]$ for a time duration $\hat{t}_{D_1D_2} - 2/(\hat{q}_s\hat{u}_n)$, which decreases as $\hat{v}_{\text{cut}}$ increases. That is, the cost $\mathrm{E}[\hat{\Delta}_{OD}]$ increases as $\hat{v}_{\text{cut}}$ increases. Hence, the free-flow branch bounded by cuts $R^i(\hat{v}^i_{\text{cut}}, \hat{k}) = \mathrm{E}[\hat{\Delta}_{OD}] + \hat{k} \cdot \hat{v}^i_{\text{cut}}$ underestimates the free flow $\mathbf{Q}$, especially when $\hat{v}_{\text{cut}} \to \hat{\mathbf{V}}_f$. The free-flow branch should be concave, which will be approximated in Section 5.3.

5.2. Wave speed for $k = \hat{k}_0$

In Figure 7(b), a moving observer moves from 'O' to 'D'. The slope of line $O \to D$ is $-\hat{v}_{\text{cut}}$, which is limited in $[-\hat{w}, 0)$. The cost along path $O \to D_3$ and the path $D_4 \to D$ are $\hat{k}_j \hat{w}$. The cost along path $D_3 \to D_4$ is $\mathrm{E}[\hat{\mathbf{C}}^-]$. Hence, the average cost from 'O' to 'D' is equal to $[\hat{k}_j + \mathrm{E}[\hat{\mathbf{C}}^-] \cdot (1/\hat{v}_{\text{cut}} - 1/\hat{w})] \cdot \hat{v}_{\text{cut}}$. When two cuts intersect at $\hat{k}^{ij}$ ($i, j = 1, 2 \cdots m$ and $i \neq j$), we can have $\hat{k}^{ij} = \hat{k}_j - \mathrm{E}[\hat{\mathbf{C}}^-]/\hat{w}$.

Consider a case that $\lim_{\text{ø} \to 0} \hat{v}_{\text{cut}} = \hat{w} - \text{ø}$, (i.e. the time duration between D_3 and D_4 is close to zero). The probability that the moving observer meets one cyclist at location $\hat{x} = \hat{L}_s$ is close to zero. That is, there are two possibilities: i) moving observer will meet at least one cyclist when traveling at speed $-\hat{w}$ on the shared lane, or ii) the moving observer will meet no cyclist at all when moving on the shared lane. If the moving observer can meet one cyclist on the shared lane, the moving observer can fully use the cyclist trajectory, traveling at speed $\hat{v}_s$ to moving downstream (recall that the path where moving observer can fully use the cyclist trajectory to move downstream is defined as Path 1), to give the cost associated with the horizontal segment. If the moving observer does not meet any cyclist, the cost on the horizontal segment should be $\hat{c}$. That is, the cost in $D_3 \to D_4$ should be either $\hat{C}_1$ or $\hat{c}$ on condition that $\lim_{\text{ø} \to 0} \hat{v}_{\text{cut}} = \hat{w} - \text{ø}$.

Now we calculate the probability that the moving observer will meet the cyclist on the shared lane section. Consider a second moving observer that moves *backward* in time from D_3 (i.e. moves left horizontally) at $x = \hat{L}_s$, see Figure 7(b). Consider a time duration $\hat{W}_b$. The second moving observer meets a cyclist after moving for $\hat{W}_b$. See an example shown in Figure 7(b), the second moving observer trajectory intersects with line OD_3 at point I. If the point I overlaps with the point O, we can see that $\hat{W}_b = (\hat{L} - \hat{L}_s)(1/\hat{v}_s + 1/\hat{w})$. If the first moving observer (which moves forward in time on Path $O \to D_3 \to D_4 \to D$) does not meet any cyclist when traveling from O to D_3, the time duration $\hat{W}_b$ should be longer than $(\hat{L} - \hat{L}_s)(1/\hat{v}_s + 1/\hat{w})$. Recall that $\hat{W}_b$ shows an exponential distribution with $\mathrm{E}[\hat{W}_b] = 1/(\hat{q}_s \hat{u}_n)$. Hence, on condition that $\lim_{\text{ø} \to 0} \hat{v}_{\text{cut}} = \hat{w} - \text{ø}$, the probability of $\hat{\mathbf{C}}^- = \hat{c}$ is $1 - \mathrm{P}(\hat{W}_b \leqslant (\hat{L} - \hat{L}_s)(1/\hat{v}_s + 1/\hat{w}))$ and the probability of $\hat{\mathbf{C}}^- = \hat{C}_1$ is $\mathrm{P}(\hat{W}_b \leqslant (\hat{L} - \hat{L}_s)(1/\hat{v}_s + 1/\hat{w}))$. Therefore, if $\hat{v}_{\text{cut}} = \hat{w} - \text{ø}$ where $\text{ø} \to 0$, $\mathrm{E}[\hat{\mathbf{C}}^-] = (1 - \mathrm{e}^{-\hat{u}_n \beta_1 \beta_2}) \cdot \frac{1}{\beta_1} + \hat{c} \cdot \mathrm{e}^{-\hat{u}_n \beta_1 \beta_2}$ which is smaller than $\mathrm{E}[\hat{C}]$. Decreasing $\hat{v}_{\text{cut}}$ will increase $\mathrm{E}[\hat{\mathbf{C}}^-]$ and decrease $\hat{k}_{ij}$ as well. Therefore we construct a series of cuts as shown in Figure 8. A bold line shows the FD shaped by those cuts. We can see that $\mathrm{d}\hat{\mathbf{Q}}/\mathrm{d}\hat{k} = -\hat{w}$ for $k = \hat{k}_0$.

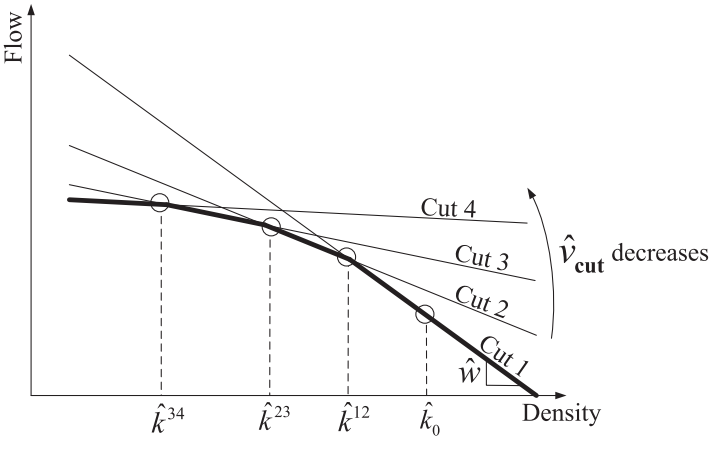

Figure 8. Wave speed for $\hat{k} = \hat{k}_0$.

5.3. Fundamental diagram approximation

We simply try a second order expression to formulate the FD free-flow branch as

$$\hat{\mathbf{Q}}(\hat{k}) = \hat{\mathrm{C}}\left[\frac{\theta_1 \hat{k}}{\hat{\mathbf{K}}_c} + (1-\theta_1)\left(\frac{\hat{k}}{\hat{\mathbf{K}}_c}\right)^{\theta_1/(\theta_1-1)}\right] \quad \text{when } \hat{k} \in \left[0, \hat{\mathbf{K}}_c\right] \tag{8}$$

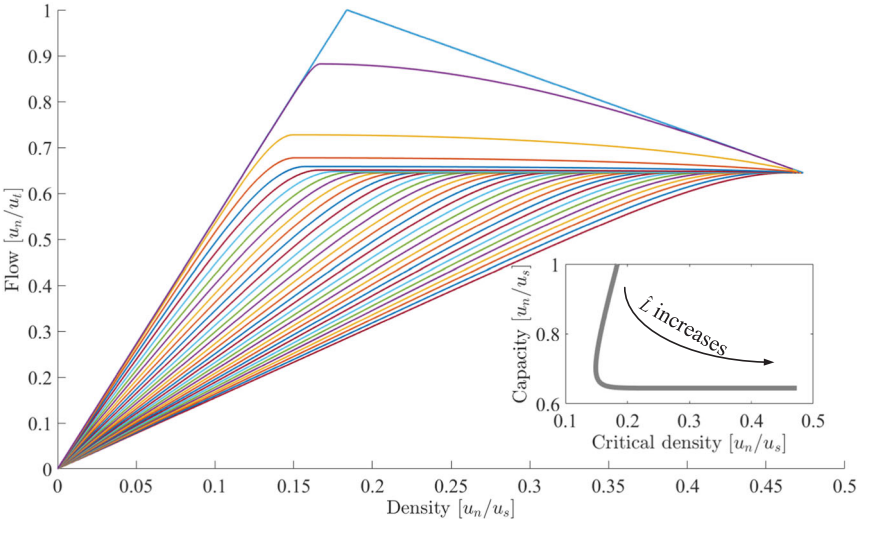

(a)

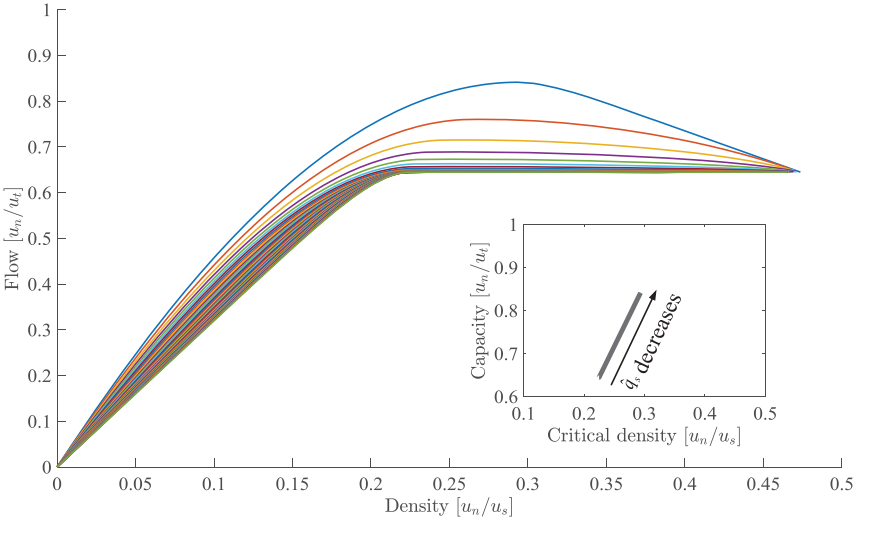

(b)

Figure 9. Sensitivity of fundamental diagram to (a) $\hat{L}$ and (b) $\hat{q}_s$. (a) FD corresponding to different $\hat{L}$. The subfigure at the right corner shows the capacity–critical density plot, showing how the FD changes as $\hat{L}$ increases. When $L/L_s = 1$, the FD is the same as the triangular fundamental diagram. The cyclist flow $\hat{q}_s = 0.0125$ and the bike lane length $\hat{L}_s \approx 1.36$. (b) FD corresponding to different $\hat{q}_s$. The subfigure at the right corner shows the capacity–critical density plot, showing how the FD changes as $\hat{q}_s$ decreases. The ring road length $\hat{L} \approx 1.94$ and the bike lane length $\hat{L}_s \approx 1.36$.

and the congestion branch is

$$\hat{\mathbf{Q}}(\hat{k}_0-\hat{k})=\left(\hat{\mathrm{C}}-\hat{k}_0\hat{v}_s\right)\left[\frac{\theta_2\hat{k}}{\hat{k}_0-\hat{\mathbf{K}}_c}+(1-\theta_2)\left(\frac{\hat{k}}{\hat{k}_0-\hat{\mathbf{K}}_c}\right)^{\theta_2/(\theta_2-1)}\right]+\hat{k}_0\hat{v}_s \tag{9}$$

where $\hat{k}\in[\hat{\mathbf{K}}_c,\hat{k}_0]$, $\theta_1=\hat{\mathbf{K}}_c\hat{\mathbf{V}}_f/\hat{\mathbf{C}}$ and $\theta_2=(\hat{k}_0-\hat{\mathbf{K}}_c)\hat{w}/(\hat{\mathrm{C}}-\hat{k}_0\hat{v}_s)$. This second order equation has been used in Daganzo and Knoop (2016) for the FD approximation on pedestrianized streets, which is claimed to fit for simulation results well.

Given $\hat{q}_s$, the close-form analytical equations proposed in this work, including (1), (5) and (7), show that the FD is a single-parameter function of $\hat{L}$.

Using (8) and (9), we present FDs given different $\hat{L}$, see Figure 9(a). In the subfigure in Figure 9(a), the FD capacity and its corresponding critical density is plotted, which also sheds light on how the FD changes corresponding to different $\hat{L}$. In Figure 9(b), the sensitivity of FD to the $\hat{q}_s$ is also presented. As the cyclist flow increases, the capacity and the critical density will decrease and increase, respectively.

6. Simulations

This section compares the FD predicted in Section 2 with simulations. We use Newell's car-following model to simulate vehicles. Nature units are used in simulations. Traffic is described with a triangular fundamental diagram (free-flow speed $v_f=80$ km/h, $k_c=20$ veh/km and $w=18$ km/h). The number of cyclists $n=10$ veh and the cyclist speed $v_s=20$ km/h. The ring road length is $L=10$ km and the bike lane length L_s is variable. In simulations in this work, we consider $L_s=3$, 5, 7 and 9 km. The initial locations of cyclists on the ring road are generated randomly from a single uniform distribution. The initial spacing of each vehicle is equal to L/n. The time step is $3600/(wk_j)\approx 1.8$s. The simulation time is around 750 min for one run.

Figure 10 shows simulated traffic trajectories on the ring road as an example ($L_s=5$ km). The lines are the vehicular trajectories, while the dots show the cyclist trajectories. Dots are absent between $x=0$ km and $x=5$ km since cyclists are traveling on the bike lane. The road structure is the same as shown in Figure 1(a). When vehicles meet cyclists, they will slow down to v_s until the cyclist enters the bike lane.

According to Edie's traffic flow measurement definition (Edie 1963), the flow is calculated as the ratio of total distance traveled by all vehicles in a spatial-temporal window, and the area of the window.

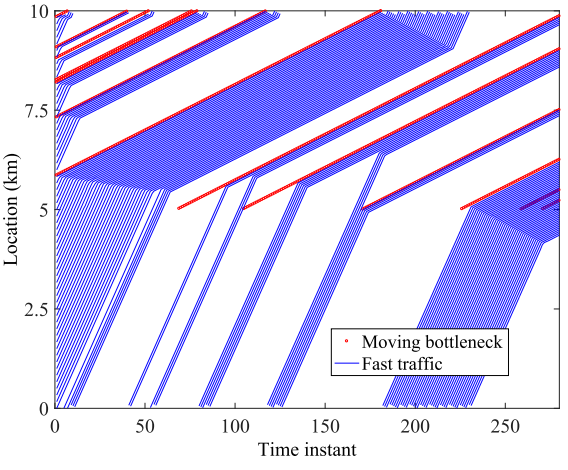

Figure 10. Traffic trajectories in simulations.

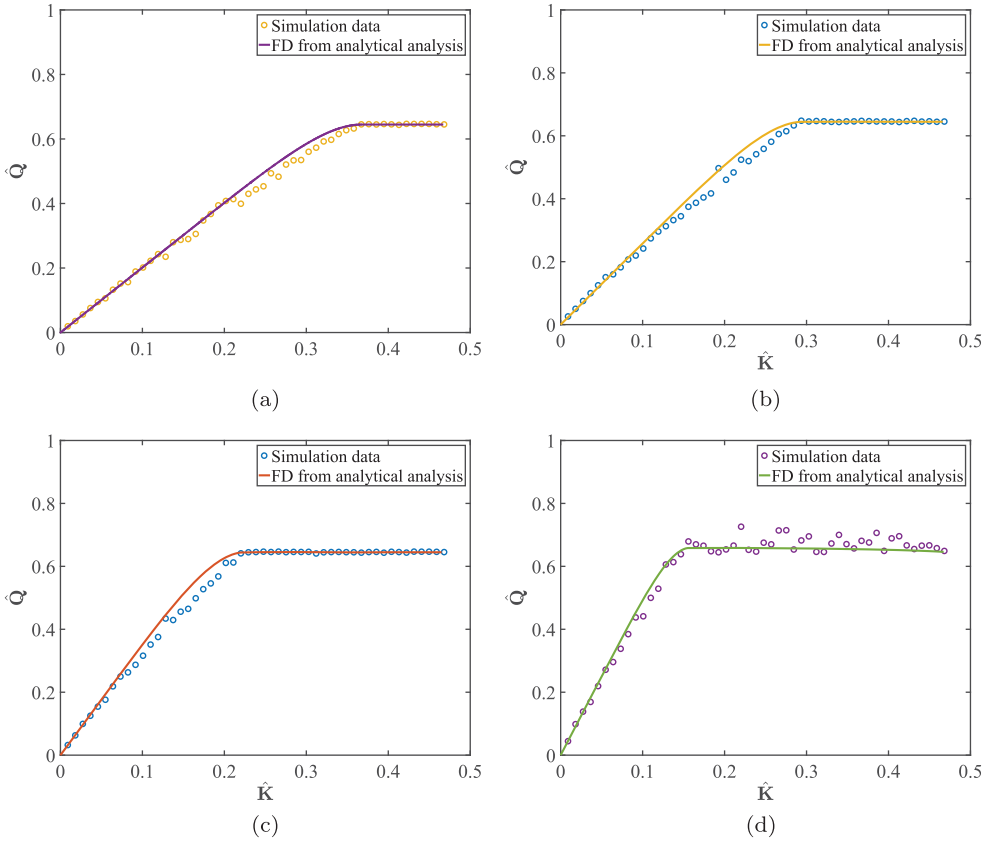

Figure 11. A comparison of FD between the simulation results and the analytical analysis, with $\hat{L}$ approximated as (a) 4.5, (b) 2.7, (c) 1.9 and (d) 1.5.

To discard any initial transient, the flow in the first 100 min is not considered. With a same $\hat{L}$, we simulate 51 densities in total (i.e. $\hat{\mathbf{K}} = 1, 2, \ldots, 51$ veh/km), with one run per density.

Figure 11 compares the FD from simulations with the FD produced from (8) and (9). The FD from simulations is shown as circles. The solid line shows the FD produced from analytical formulas. The results are shown in dimensionless units. $\hat{L} = \{4.5, 2.7, 1.9, 1.5\}$ corresponds to $L_s = \{3, 5, 7, 9\}$ km or bike lane proposition $L_s/L \cdot 100\% = \{30\%, 50\%, 70\%, 90\%\}$. From Figure 11, we argue that the analytic results are able to present the main characteristics of the simulation results (e.g. capacity, free-flow speed and critical density).

7. Traffic flow with overtaking probability on shared lanes

In this section, we focus on extending the FD on a single-shared lane street to that on a multi-lane street. On a multi-lane road, vehicles can pass the cyclists even without a bike lane. Figure 12 shows a studied multi-lane road structure. Different from Figure 1(a), vehicles can overtake cyclists on the passing lanes. Cyclists will share the shoulder lane when there is no bike lane, unless there is a bike lane. Vehicles can drive on all lanes except the bike lane. According to the behavioral theory of multi-lane traffic flow in Daganzo (2002), this research makes an assumption about the driver behavior as follow:

- Assumption 5: Vehicles as rabbits that always drive on the lanes with the highest speed, while cyclists as slugs that do not travel on the passing lanes.

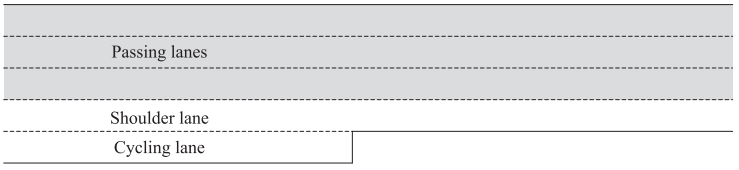

Figure 12. Studied multi-lane road structure.

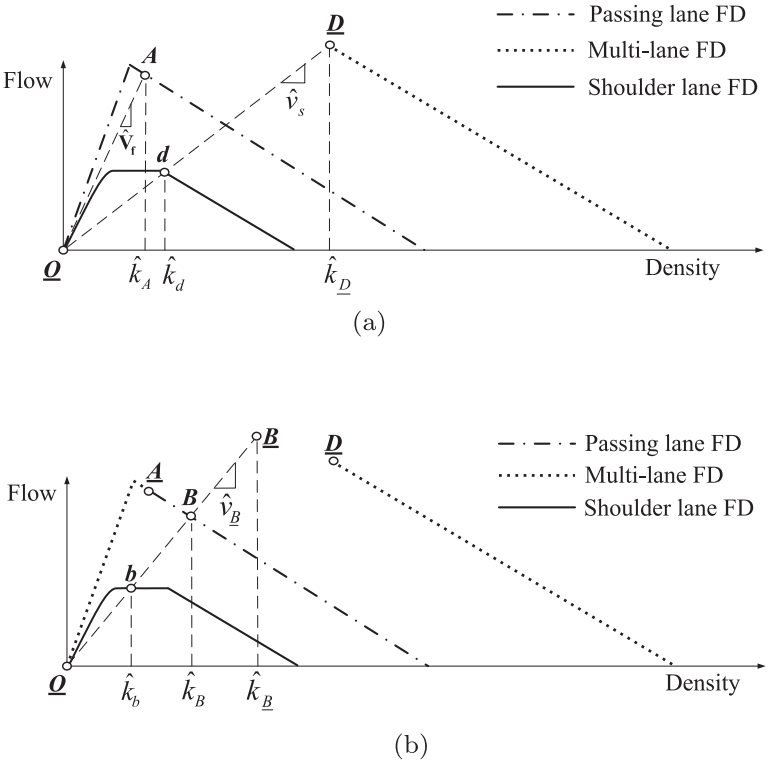

Figure 13. Giving possible stationary traffic states on a multi-lane road. (a) Stationary traffic states on the passing lane, shoulder lane and the whole multi-lane road. (b) Approaches to give possible stationary traffic states on the whole multi-lane road.

That is, only when the speed on the shoulder lane is not lower than that on the passing lanes, vehicles will enter the shoulder lane with a probability. The assumption 6 obeys a user-equilibrium principle, stating that no driver can unilaterally reduce the travel time by shifting to another lane. During a certain density range, the travel time on the shoulder lane should be independent of the total traffic density and other lanes. It is not straightforward to use the approach proposed to the no-overtaking problem to solve the multi-lane problem.

Figure 13 shows stationary traffic states on the passing lane (dot-dash line), the shoulder lane (bold line) and the whole multi-lane road (dotted line). The jam density on the passing lane is 3 in this work because the number of passing lanes is three, the free-flow speed and the wave speed are the same as $\hat{v}_f$ and $\hat{w}$, respectively. The stationary states on the passing lane are indicated by capital letters. The stationary traffic states on the shoulder lane are shown according to (8) and (9), indicated by small letters. The stationary traffic states on the multi-lane road are indicated by underlined capital letters. Density is described as $\hat{k}$, whose subscript corresponds to the stationary traffic states.

When the vehicular density is rather small (e.g. the passing lanes are empty), vehicles will only drive on the passing lanes. In Figure 13(a), the vehicular speed corresponding to state A is the free-flow speed on the shoulder lane $\hat{\mathbf{V}}_{\mathrm{f}}$. Recall that $\hat{\mathbf{V}}_{\mathrm{f}} < \hat{v}_f$ due to cyclists (see Section 4). As the density is lower than $\hat{k}_A$, the vehicular speed on passing lanes is always higher than $\hat{\mathbf{V}}_{\mathrm{f}}$, which means all vehicles will choose to drive on the passing lanes for a higher speed. That is, the FD within density range $[0, \hat{k}_A]$ on the multi-lane road should be the same as the FD on the passing lanes. Graphically, in Figure 13(b) on the left of state A, we use dotted line (corresponding to multi-lane road stationary states) to replace the dot-dash line in Figure 13(a). The state A is replaced by $\underline{A}$ ($\hat{k}_A = \hat{k}_{\underline{A}}$).

When the road density is higher than $\hat{k}_{\underline{A}}$, the vehicular speed on the passing lane will be lower than $\hat{\mathbf{V}}_{\mathrm{f}}$ unless a proportion of vehicles place themselves on the shoulder lane, which will synchronize the traffic speed on all lanes including passing lanes and the shoulder lane. The space on the shoulder lane will be used. Hence, within some certain density range, the total flow on the multi-lane road can increase again, while the vehicular density rise and the speed decreases.

Let $\hat{k}_d = \hat{k}_0$ with corresponding vehicular speed $\hat{v}_s$. As the road density is higher than $\hat{k}_{\underline{D}} = 4\hat{k}_0$, cyclists are not moving observer at all since the cyclist speed is also influenced by vehicles. The stationary traffic states should lie on a straight line with slope $-\hat{w}$ and the jam density is 4, see the dotted line in both Figure 13(a) and (b).

When figuring out the stationary states within density range $[\hat{k}_{\underline{A}}, \hat{k}_{\underline{D}}]$, we can draw a dashed line $\underline{O} - \underline{B}$ indicating a traffic speed $\hat{v}_{\underline{B}}$, see Figure 13(b). When the vehicular speed is $\hat{v}_{\underline{B}}$, the traffic state

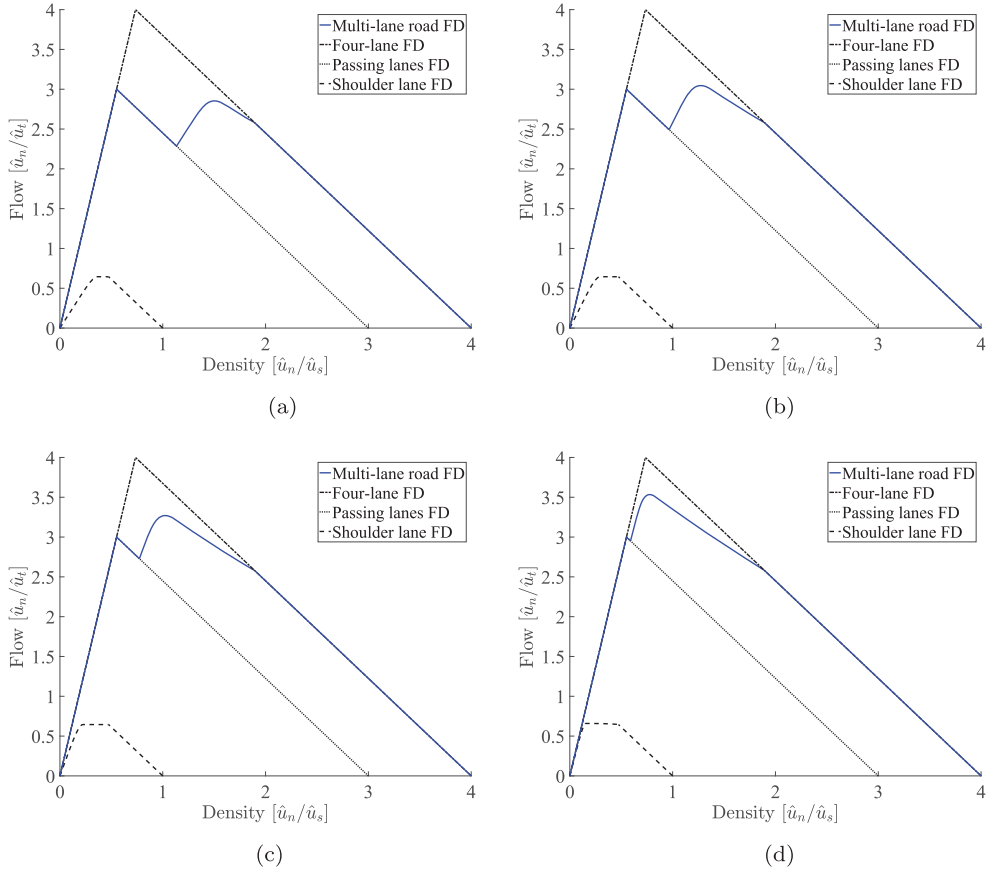

Figure 14. Stationary traffic states on the multi-lane road with one lane partly shared with cyclists with $\hat{q}_s = 0.0125$. (a) $\hat{L} = 4.5$, (b) $\hat{L} = 2.7$, (c) $\hat{L} = 1.9$ and (d) $\hat{L} = 1.5$.

on the shoulder lane and the passing lane is b and B, respectively. State $\underline{B}$ denotes the overall traffic state on the multi-lane road. The density on the road is $\hat{k}_{\underline{B}} = \hat{k}_B + \hat{k}_b$, where $\hat{k}_B = 3\hat{w}/(\hat{v}_{\underline{B}} + \hat{w})$ and $\hat{v}_{\underline{B}} = \hat{\mathbf{Q}}(\hat{k}_b)/\hat{k}_b$. Hence, we can express the $\hat{k}_{\underline{B}}$ and $\hat{q}_{\underline{B}}$ as functions of $\hat{k}_b$,

$$\hat{k}_{\underline{B}} = \frac{3\hat{w}\hat{k}_b}{\left(\hat{\mathbf{Q}}(\hat{k}_b) + \hat{w}\hat{k}_b\right)} + \hat{k}_b \tag{10}$$

and

$$\hat{q}_{\underline{B}} = \frac{\hat{k}_{\underline{B}}\hat{\mathbf{Q}}(\hat{k}_b)}{\hat{k}_b} \tag{11}$$

By calculating the $(\hat{k}_{\underline{B}}, \hat{q}_{\underline{B}})$ corresponding to every $\hat{k}_b$ using (10) and (11), we can give the multi-lane road fundamental diagram. Figure 14 shows the multi-lane road FD with different $\hat{L}$. In all subfigures in Figure 14, the four-lane FD indicates the density-flow fundamental diagram on a four-lane road section without disruptions from cyclists. In Figure 14, the cyclist flow is a constant, $\hat{q}_s = 0.0125$.

As shown in Figure 14, the FD shows a two-peak shape. As the $\hat{L}$ decreases (i.e. L_s/L increases up close to 1), the multi-lane FD will be more close to the four-lane FD. If the bike lane length proportion is high enough, the road capacity will be determined by the shoulder lane capacity. Otherwise, the capacity will be minimized to the passing-lane road capacity, independent of the shoulder lane traffic flow. In Figure 14, when the bike lane length proportion is below about 50% (and $\hat{q}_s = 0.0125$), the capacity of the whole road is equal to the passing lane capacity.

8. Conclusions

This work studies the traffic flow on a road which is partly shared by passenger cars and cyclists. Cyclists will only cycle on the bike lane until the end of the bike lane where they will merge into the shared lane. This work focuses on the impacts of the bike lane length proportion and the cyclist flow on the traffic flow on streets in a linkwise.

We firstly study the FD on a one-lane road which is partly covered by a bike lane. Close-form formulas show how the FD is affected by the bike lane length and the cyclist flow. Secondly, we extend the FD on the one-lane road to the FD on a multi-lane road. The shoulder lane is partly shared by the cyclists and the passage cars. Vehicles can overtake cyclists on the shared road section. Applying the multi-lane behavioral theory from Daganzo (2002), we predict the stationary traffic states on a multi-lane road.

The spacing occupied by the slow traffic is not counted. In the future, the space occupied by slow traffic should be taken into considerations following which we can estimate the mixed traffic flow. Besides, because the slow traffic can be considered as other traffic modes such as buses or heavy trucks, this work can be extended in the future to include the interactions among different types of road users. Finally, this work only studies the traffic flow in a linkwise. Further extension to traffic flow dynamics in a network wise is desirable in the future.

Disclosure statement

No potential conflict of interest was reported by the authors.

ORCID

Serge P. Hoogendoorn http://orcid.org/0000-0002-1579-1939

References

Chen, Danjue, Soyoung Ahn, Soohyuk Bang, and David Noyce. 2016. "Car-Following and Lane-Changing Behavior Involving Heavy Vehicles." *Transportation Research Record: Journal of the Transportation Research Board* 2561: 89–97. http://dx.doi.org/10.3141/2561-11.

Coifman, Benjamin. 2015. "Empirical Flow-Density and Speed-Spacing Relationships: Evidence of Vehicle Length Dependency." *Transportation Research Part B: Methodological* 78: 54–65.

Daganzo, Carlos F. 2002. "A Behavioral Theory of Multi-Lane Traffic Flow. Part I: Long Homogeneous Freeway Sections." *Transportation Research Part B: Methodological* 36 (2): 131–158.

Daganzo, Carlos F. 2005. "A Variational Formulation of Kinematic Waves: Basic Theory and Complex Boundary Conditions." *Transportation Research Part B: Methodological* 39 (2): 187–196.

Daganzo, Carlos F., and Nikolas Geroliminis. 2008. "An Analytical Approximation for the Macroscopic Fundamental Diagram of Urban Traffic." *Transportation Research Part B: Methodological* 42 (9): 771–781.

Daganzo, Carlos F., and Victor L. Knoop. 2016. "Traffic Flow on Pedestrianized Streets." *Transportation Research Part B: Methodological* 86: 211–222.

Edie, Leslie C. 1963. "Discussion of Traffic Stream Measurements and Definitions." Proceedings of the 2nd International Symposium on the Theory of Road Traffic Flow, France, 139–154.

HCM. 2016. *Highway Capacity Manual 6th Edition: A Guide for Multimodal Mobility Analysis*. Washington DC: Transportation Research Board.

Hoogendoorn, Serge, and Winnie Daamen. 2016. "Bicycle Headway Modeling and Its Applications." *Transportation Research Record: Journal of the Transportation Research Board* 2587: 34–40.

Knoop, V. L., and C. F Daganzo. 2017. "The Effect of Pedestrian Crossings on Traffic Flow." Inproceedings of the 96th Annual Meeting of the Transportation Research Board.

Laval, Jorge. 2006a. "Stochastic Processes of Moving Bottlenecks: Approximate Formulas for Highway Capacity." *Transportation Research Record: Journal of the Transportation Research Board* 1988: 86–91. https://doi.org/10.3141/1988-13.

Laval, Jorge A. 2006b. "A Macroscopic Theory of Two-Lane Rural Roads." *Transportation Research Part B: Methodological* 40 (10): 937–944.

Laval, Jorge A. 2009. "Effects of Geometric Design on Freeway Capacity: Impacts of Truck Lane Restrictions." *Transportation Research Part B: Methodological* 43 (6): 720–728.

Laval, Jorge A., and F. Daganzo Carlos. 2006. "Lane-Changing in Traffic Streams." *Transportation Research Part B: Methodological* 40 (3): 251–264.

Leclercq, Ludovic, Jorge A. Laval, and Nicolas Chiabaut. 2011. "Capacity Drops at Merges: An Endogenous Model." *Transportation Research Part B: Methodological* 45 (9): 1302–1313.

Muñoz, J. C., and C. F Daganzo. 2002. "Moving Bottlenecks: A Theory Grounded On Experimental Observation." Proceedings of the 15th International Symposium on Transportation and Traffic Theory, 441–461.

van Wageningen-Kessels, Femke. 2013. "Multi-Class Continuum Traffic Flow Model: Analysis and Simulation Methods." PhD thesis, Delft University of Technology.

van Wageningen-Kessels, Femke. 2016. "Framework to Assess Multiclass Continuum Traffic Flow Models." *Transportation Research Record: Journal of the Transportation Research Board* 2553: 150–160. http://dx.doi.org/10.3141/2553-16.

Wong, G. C. K, and S. C. Wong. 2002. "A Multi-Class Traffic Flow Model: An Extension of LWR Model with Heterogeneous Drivers." *Transportation Research Part A: Policy and Practice* 36 (9): 827–841.